Electrochemistry Communications 49 (2014) 38–41

Contents lists available at ScienceDirect

Electrochemistry Communications

journal homepage: www.elsevier.com/locate/elecom

Short communication

Solvent co-deposition during oxygen reduction on Au in DMSO $LiPF_6$

W.R. Torres, A.Y. Tesio, E.J. Calvo *

INQUIMAE, Facultad de Ciencias Exactas y Naturales, Pabellón 2, Ciudad Universitaria, AR-1428 Buenos Aires, Argentina

ARTICLE INFO

Article history:
Received 13 August 2014
Received in revised form 17 September 2014
Accepted 22 September 2014
Available online 28 September 2014

Keywords:
Lithium air batteries
ORR
Superoxide
Lithium peroxide
EQCM

ABSTRACT

Rotating ring disk electrode (RRDE) and electrochemical quartz crystal microbalance (EQCM) have been employed for chronoamperometry of the oxygen reduction reaction (ORR) on gold electrodes in O_2 saturated $LiPF_6$/DMSO electrolyte. The Au ring electrode ($E_R = 3.0$ V) detects a small fraction of soluble superoxide generated at the disk while EQCM detects the mass of ORR insoluble products. By integration of the ORR current transient the mass to charge plots exhibit mass per electron (mpe) values which largely exceed those expected for simple O_2 to O_2Li or Li_2O_2 reactions. Therefore the co-deposition of solvent and/or side reactions such as electrolyte degradation should be taken into consideration to explain the experimental evidence.

1. Introduction

There is a very active search for suitable electrolytes for the rechargeable lithium–air battery which has a very large theoretical energy density competitive with fossil fuels for electric vehicle applications with extended millage range [1–5]. Ogasawara et al. [6] have shown that the electrochemical reaction of Li^+ with oxygen yields insoluble Li_2O_2 in non-aqueous electrolyte. Peng et al. [7] claimed that the Li–air battery can be recharged with 95% capacity retention in 100 cycles using dimethyl sulfoxide (DMSO) electrolyte and porous gold electrode in DMSO. There is, however, controversy on the stability of DMSO in the presence of oxygen reduction reaction (ORR) products [8] in particular when the electrode area to electrolyte volume is high [9]. Furthermore, solid $LiPF_6$ has been shown to react with Li_2O_2 by XPS [10].

Rotating ring disk electrode (RRDE) studies failed to detect soluble superoxide ion in acetonitrile with 0.1 M $LiPF_6$ [11]. However in DMSO electrolyte re-oxidation of O_2^- can be detected in fast cyclic voltammetry if the cathodic excursion is limited so that further reduction or disproportionation of superoxide is avoided [12]. In DMSO lithium containing solutions, soluble lithium superoxide has been detected at the ring electrode [11] and in acetonitrile $LiClO_4$ solutions with only 0.1 M DMSO soluble lithium superoxide could be detected with a rotating ring disk electrode [13].

On the other hand, a few studies with the electrochemical quartz crystal microbalance (EQCM) have been disclosed for this cathodic electrode process. Uosaki et al. [14] have recently reported EQCM studies of O_2 reduction in $LiPF_6$-DMSO electrolyte deposition on a gold electrode. These authors reported the mass per electron (mpe) calculated from the slope of a mass-to-charge plot of 37 g/mol-e in a very limited potential window of the ORR, suggesting deposition of lithium superoxide (LiO_2). Aurbach et al. [9,15] reported on similar EQCM studies with an mpe of 22 g/mol-e in the limited voltage interval of 2.7 to 2.3 V and larger values that correspond to DMSO decomposition products of larger molar mass.

In the present communication we present some preliminary results of rotating ring disk electrode (RRDE) and electrochemical quartz crystal microbalance (EQCM) in chronoamperometry of the oxygen reduction reaction (ORR) on gold electrodes in O_2 saturated $LiPF_6$/DMSO electrolyte. These studies disclose new evidence of mass per electron deposited that cannot be explained by simple oxygen to lithium superoxide and peroxide reactions and it is suggested that dimethylsulfoxide is co-deposited with the oxygen reduction products leading to decomposition products of higher molar mass.

2. Experimental

Anhydrous dimethyl sulfoxide (DMSO), ≥99.9% (SIGMA-ALDRICH), and $LiPF_6$ battery grade, ≥99.99%, were stored in the argon-filled MBRAUN glove box with the oxygen content ≤ 0.1 ppm and water content below 2 ppm. DMSO was dried for several days over molecular sieves, 3 Å (SIGMA-ALDRICH). All solutions were prepared inside the glove box and the water content was measured using the Karl Fisher 831 KF Coulometer (Metrohm) with typically 50 ppm of water. Since long term experiments in lithium electrolyte accumulated water from the ambient, short term experiments with freshly prepared solutions and short exposure to dry air were preferred. It should be mentioned that 50 ppm traces of water (c.a. 3 mM) may affect the stability of superoxide ion since its concentration at the electrode surface is of similar magnitude. Protonation of O_2^- would promote the fast disproportionation of HO_2.

* Corresponding author. Tel.: +54 11 4576 3380.
E-mail address: calo@qi.fcen.uba.ar (E.J. Calvo).

http://dx.doi.org/10.1016/j.elecom.2014.09.017
1388-2481/

Au/Au rotating ring disk electrode embedded in Araldite epoxy resin (Ciba-Geigy) cylindrical body with disk radius $r_1 = 0.25$, inner and outer radii ($r_2 = 0.26$ and $r_3 = 0.30$) was employed. The geometric collection efficiency $N_0 = 0.29$ was calculated using the Albery–Hitchman theory [16] and experimentally verified with the $Fe(CN)_6^{4/3-}$ redox couple in a galvanostatic experiment $N_0^{exp} = 0.28$. The disk electrode area was 0.2 cm^2.

Electrochemical experiments were performed in an air-tight acrylic box filled with Ar and dried with phosphorous pentoxide keeping a positive pressure by a stream of dry oxygen. The motor controller, motor and disk, and ring mercury contacts in the bearing block are located outside the air-tight acrylic box and sealed with a rubber ring with a permanent flow of dry oxygen in the box. The air tight box contained also the RRDE cylinder immersed in the aprotic electrolyte in a four-electrode glass cell; the electrolyte was fed from bottles filled in the glove box by a system of needles and Teflon tubes without contact with the atmosphere. Large area platinum gauze was used in a compartment separated from the main compartment by a fritted glass.

A non-aqueous Ag/Ag^+ reference electrode was used in a fritted glass compartment filled with a 0.01 $AgNO_3$ solution in 0.1 M TBA PF_6^- acetonitrile. The electrode potential of 3.7 V vs. Li/Li^+ (3.2 mm diameter Li wire, 99.9% trace metals basis ALDRICH, in the Ar filled glove box, in contact with 0.1 $LiPF_6$ in DMSO) was measured, and all potentials herein are referred to the Li/Li^+ scale.

The EQCM experiments have been described elsewhere [17], in brief: A complex voltage divider reported elsewhere was used to measure the resonance frequency and both components of the quartz crystal modified Butterworth–Van Dyke (lumped-element BVD) equivalent circuit. This device operates by applying to the quartz crystal a 10 MHz sinusoidal voltage (5 mV peak-to-peak) generated by a voltage-controlled oscillator (VCO) connected to the D/A output of a data acquisition system. Both input (*Vi*) and output (*Vo*) ac voltage moduli were amplified and rectified, and the resulting signals were measured with an A/D converter under computer control. The ratio of the circuit transfer function modulus, that is, $|V_o/V_i|$ as a function of the VCO output signal frequency was fitted to the nonlinear analytical equation of the BVD transfer function, and the equivalent circuit elements *L*, *R*, C_0 and *C* were obtained. For low crystal load by the surface deposit ($Z_L \ll Z_Q$) a lumped element circuit can be approximated and the shift in the quartz impedance due to the ORR products deposit can be written: $\Delta Z = \Delta R + j\Delta(\omega L)$, where ΔR and $\Delta(\omega L)$ are the real and imaginary parts of the impedance shift with respect to the initial quartz crystal condition. Thus, equivalent to the Saurbrey equation that relates the resonant frequency with the areal mass of deposit: $\Delta f = -\frac{(2f_0^2)}{\sqrt{(\rho_Q \mu_Q)}} \cdot \frac{\Delta m}{A}$ which applies for acoustically thin films ($R \to 0$), we have: $\Delta(\omega L) = \Delta X_L = -\frac{\pi Z_Q \Delta f}{f_o} = \frac{2\pi Z_Q \Delta m}{\sqrt{(\rho_Q \mu_Q)A}}$.

Therefore, the quartz resonator resonance frequency responds both to changes in the inertial mass as well as viscoelastic changes of the liquid electrolyte in contact with the quartz crystal and the surface deposit. For acoustically thin films ($\Delta R \ll \Delta(\omega L)$) changes in resonant frequency or $\Delta(\omega L)$ can be related to changes in the mass per unit area deposited on the Au coated quartz crystal. Calibration of the EQCM was done with electrochemical deposition of silver and the operational conversion factor used is $5.3 \times 10^{-8}\ g \cdot \Omega^{-1} \cdot cm^{-2}$.

3. Results and discussion

In oxygen saturated 0.1 M 0.1 $LiPF_6$ in DMSO the electrochemical oxygen reduction takes place in the potential range of 2.75 to 1.8 V with passivation of the Au electrode surface by oxygen reduction products [12]. Fig. 1 depicts a rotating ring disk electrode (RRDE) chronoaperometric transient of a Au electrode at 2.0 V in the ORR potential range and the simultaneous collection of soluble lithium superoxide at the Au ring electrode poised at 3.0 V. While the ORR disk current decays first to a constant current and then drops to zero, the O_2^- oxidation ring current goes through a maximum, then follows a constant disk current and finally dies away as the disk current does. Notice that the ring current normalized by the geometric collection efficiency measures the flux of soluble lithium superoxide species at the disk electrode surface and represents only a small fraction of the total ORR disk current since most of the charge is accumulated as ORR surface products as confirmed by EQCM.

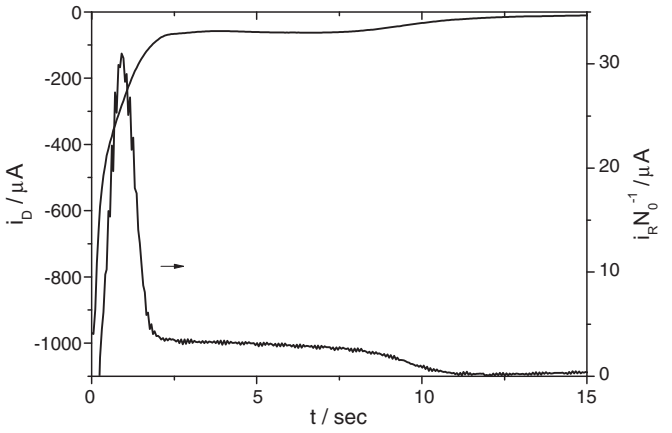

Fig. 1. Chronoamperometry for the ORR on Au/Au RRDE in O_2 saturated 0.1 M $LiPF_6$ DMSO electrolyte and the simultaneous ring current normalized by the collection efficiency. $E_D = 2.0$ V $E_R = 3.0$ V. W = 9 Hz.

The disk current transient results from the ORR on the Au surface partly covered by an in-soluble insulating Li_2O_2 deposit that progressively blocks the electron transfer at the surface. In the constant current region, it appears that the oxygen reduction still can proceed on a Li_2O_2 thin film but at a lower rate until a critical peroxide film thickness is reached. Simultaneous to the disk current transient, a ring current transient after the peak follows the disk current and the superoxide flux at the disk (I_R/N_0) is only 10% of the disk current so that the fraction of soluble superoxide is small. The ring current peak for the collection of superoxide ion under convective-diffusion conditions at constant disk potential exhibits a maximum at 2.2 V which can be explained by the buildup of surface LiO_2 concentration at the disk electrode with further bimolecular disproportionation at low cathodic over potentials or direct two electron reduction to Li_2O_2 at higher over potentials [18].

The electrochemical quartz crystal microbalance simultaneous to a similar chronoamperometric transient shows a mass uptake due to the deposition of O_2 reduction products as depicted in Fig. 2 under non-stirring conditions. The micrograms per square centimeter deposit

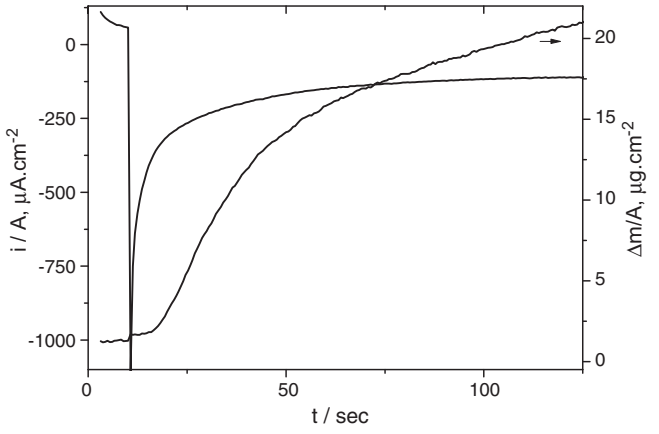

Fig. 2. Chronoamperometry for the ORR on Au/quartz EQCM in O_2 saturated 0.1 M $LiPF_6$ DMSO electrolyte. $E_D = 2.55$ V and simultaneous Δm/A.

formed during the ORR on the Au surface are much larger than the expected coverage for a lithium peroxide monolayer [19], c.a. 260 $\mu C \cdot cm^{-2}$ or 135 $ng \cdot cm^{-2}$. The morphology and quantity of Li_2O_2 deposited depend on the experimental conditions, i.e. current density or time of deposition [20].

With the EQCM derived mass and integration of the ORR current, we have obtained the mass to charge ratio and from that the mass per mole of electrons (mpe). The mpe was calculated as $\Delta m.F / \Delta Q$, with F as the Faraday constant. In Li^+ containing CH_3CN electrolyte soluble lithium superoxide could not be detected with the RRDE [11,13] and from the EQCM experiments a mass per electron of 23 g per equivalent can be derived which corresponds to a deposit of Li_2O_2 [21]. However, the almost 0.5 V difference in the $Li^{/}Li^+$ electrode potential [22] is a strong evidence of the preferential solvation of Li^+ by DMSO even at a high molar fraction of CH_3CN which would explain the high stabilization of soluble lithium superoxide.

In Fig. 3 the mass-to-charge plot corresponding to the transient in Fig. 2 exhibits two linear regions of 175 g/mol-e at short times and 61 g/mol-e at longer times. Similar slopes have also been observed in cyclic voltammetry and galvanostatic pulses in DMSO solutions of lithium salts [21]. The mpe values obtained are far too large as compared to the expected values for the ideal Li–O_2 cathode reactions indicated for the following reactions: [9]

$$O_2 + Li^+ + e \rightarrow [O_2Li]_{surf} \qquad mpe = 39 \tag{1}$$

$$O_2Li + O_2 \rightarrow Li_2O_2\downarrow + O_2 \qquad mpe = 23 \tag{2}$$

$$[O_2Li]_{surf} + Li^+ + e \rightarrow Li_2O_2\downarrow \qquad mpe = 7 \tag{3}$$

$$O_2 + 2Li^+ + 2e \rightarrow Li_2O_2\downarrow \qquad mpe = 23. \tag{4}$$

Since the molecular weight of DMSO is 78 g/mol we speculate that solvent molecules are co-deposited with either LiO_2 or Li_2O_2 which may be further decomposed at the solid/liquid interface as suggested by Aurbach et al. [9,15]. Also, some side reactions due to traces of water such as superoxide protonation and further disproportionation and partial Li_2O_2 solubilization cannot be ruled out.

At short times during the potentiostatic transient the RRDE detects a burst of soluble lithium superoxide while the EQCM detects a mass per electron too high for LiO_2 species (mpe = 39), and we speculate that the dimethylsulfoxide molecules strongly coordinated to lithium cations are co-deposited giving rise to mpe values between 115 and 200. At longer times, after the I_R peak most probably Li_2O_2 partially solvated is deposited to account for the 45–70 g per electron observed in several experiments.

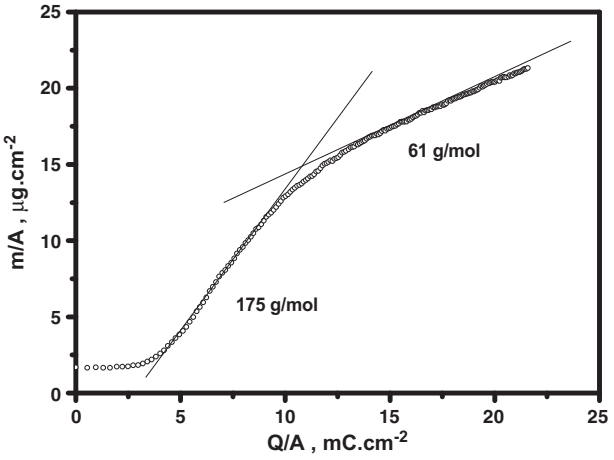

Fig. 3. Integrated mass to charge plot for chronoamperometry data in Fig. 2.

Molecular dynamic simulations of Li^+ ions in DMSO-acetonitrile mixtures have shown that for very low molar fraction four molecules of DMSO are present in the first solvation shell of Li^+ [23]. Therefore we speculate that strongly coordinated DMSO to lithium ions form $[Li^+]_{DMSO}O_2^-$ ion pairs that adsorb and then disproportionate to partly solvated Li_2O_2.

In our hands, XPS studies of the electrode surface after the ORR under similar experimental conditions have shown the presence of carbonate, organic molecules and sulfur from DMSO decomposition as well as LiF and phosphorous compounds from decomposition of PF_6^- [24]. All of these decomposition products would account for the mass in excess seen in EQCM chronoamperometric experiments. Sharon et al. [9,15] have proposed a mechanism for the decomposition of DMSO by reaction with ORR products such as LiO_2 and Li_2O_2 with the formation of a dimsyl anion-Li^+ ion pair (84 g/mol) and hydroperoxyl radical or lithium hydroperoxide radical anion pair (40 g/mol). The co-deposition of DMSO which strongly coordinated to lithium ions would be essential for its decomposition by lithium peroxide on the surface.

4. Conclusions

Rotating ring disk electrode (RRDE) and quartz crystal microbalance (EQCM) experiments simultaneous to chronoamperometry of the oxygen reduction reaction (ORR) on Au electrodes in O_2 saturated $LiPF_6$/DMSO electrolyte have produced experimental evidence for an excess mass to charge ratio of the ORR surface deposition products. Such high mass per electron can be tentatively explained by the co-deposition of dimethyl sulfoxide strongly coordinated to Li^+ ions forming ion pairs with superoxide anions, $[Li^+]_{DMSO}O_2^-$. Further formation of Li_2O_2 and heterogeneous reaction with DMSO and $LiPF_6$ would explain the XPS evidence of carbonate, fluoride, sulfur, phosphorous and organic molecules on the surface due to side reactions.

Acknowledgment

The authors acknowledge the financial support from the University of Buenos Aires, CONICET and ANPCyT grant PICT-2012-1452.

References

[1] S.A. Freunberger, Y. Chen, Z. Peng, J.M. Griffin, L.J. Hardwick, F. Barde, P. Novak, P.G. Bruce, Reactions in the rechargeable lithium–O-2 battery with alkyl carbonate electrolytes, J. Am. Chem. Soc. 133 (20) (2011) 8040–8047.
[2] P.G. Bruce, S.A. Freunberger, L.J. Hardwick, J.-M. Tarascon, Li–O-2 and Li–S batteries with high energy storage, Nat. Mater. 11 (1) (2012) 19–29.
[3] J. Christensen, P. Albertus, R.S. Sanchez-Carrera, T. Lohmann, B. Kozinsky, R. Liedtke, J. Ahmed, A. Kojic, A critical review of li/air batteries, J. Electrochem. Soc. 159 (2) (2012) R1–R30.
[4] L.J. Hardwick, P.G. Bruce, The pursuit of rechargeable non-aqueous lithium–oxygen battery cathodes, Curr. Opin. Solid State Mater. Sci. 16 (4) (2012) 178–185.
[5] K.M. Abraham, Lithium–air and other batteries beyond lithium-ion batteries, in: K.M.A. Bruno Scrosati, Walter van Schalkwijk, Jusef Hassoun (Eds.), Lithium Batteries: Advanced Technologies and Applications, First ed.John Wiley & Sons, Inc., 2013
[6] T. Ogasawara, A. Debart, M. Holzapfel, P. Novak, P.G. Bruce, Rechargeable Li_2O_2 electrode for lithium batteries, J. Am. Chem. Soc. 128 (4) (2006) 1390–1393.
[7] Z. Peng, S.A. Freunberger, Y. Chen, P.G. Bruce, Reversible and higher-rate Li–O-2 battery, Science 337 (6094) (2012) 563–566.
[8] B.D. McCloskey, A. Valery, A.C. Luntz, S.R. Gowda, G.M. Wallraff, J.M. Garcia, T. Mori, L.E. Krupp, Combining accurate O-2 and li_2o_2 assays to separate discharge and charge stability limitations in nonaqueous Li–O-2 batteries, J. Phys. Chem. Lett. 4 (17) (2013) 2989–2993.
[9] D. Sharon, M. Afri, M. Noked, A. Garsuch, A.A. Frimer, D. Aurbach, Oxidation of dimethyl sulfoxide solutions by electrochemical reduction of oxygen, J. Phys. Chem. Lett. 4 (18) (2013) 3115–3119.
[10] R. Younesi, M. Hahlin, F. Bjorefors, P. Johansson, K. Edstrom, Li–O-2 battery degradation by lithium peroxide (Li_2O_2): a model study, Chem. Mater. 25 (1) (2013) 77–84.

[11] M.J. Trahan, S. Mukerjee, E.J. Plichta, M.A. Hendrickson, K.M. Abraham, Studies of Li–air cells utilizing dimethyl sulfoxide-based electrolyte, J. Electrochem. Soc. 160 (2) (2013) A259–A267.
[12] C.O. Laoire, S. Mukerjee, K.M. Abraham, E.J. Plichta, M.A. Hendrickson, Influence of nonaqueous solvents on the electrochemistry of oxygen in the rechargeable lithium–air battery, J. Phys. Chem. C 114 (19) (2010) 9178–9186.
[13] E.J. Calvo, N. Mozhzhukhina, A rotating ring disk electrode study of the oxygen reduction reaction in lithium containing non aqueous electrolyte, Electrochem. Commun. 31 (2013) 56–58.
[14] X. Jie, K. Uosaki, Electrochemical quartz crystal microbalance study on the oxygen reduction reaction in Li + containing DMSO solution, J. Electroanal. Chem. 716 (2014) 49–52.
[15] D. Sharon, V. Etacheri, A. Garsuch, M. Afri, A.A. Frimer, D. Aurbach, On the challenge of electrolyte solutions for li–air batteries: monitoring oxygen reduction and related reactions in polyether solutions by spectroscopy and EQCM, J. Phys. Chem. Lett. 4 (1) (2013) 127–131.
[16] J.W. Albery, M. Hitchman, Rotating ring disc electrodes, Oxford University Press, Oxford, 1971.
[17] E.J. Calvo, R. Etchenique, P.N. Bartlett, K. Singhal, C. Santamaria, Quartz crystal impedance studies at 10 MHz of viscoelastic liquids and films, Faraday Discuss. 107 (1997) 141–157.
[18] W. Torres, N. MOZhzhukhina, A.Y. Tesio, E.J., C., A rotating ring disk electrode study of the oxygen reduction reaction in lithium containing dimethyl sulfoxide electrolyte: role of Superoxide, J. Electrochem. Soc. (2014) (in press).
[19] S. Meini, M. Piana, N. Tsiouvaras, A. Garsuch, H.A. Gasteiger, The effect of water on the discharge capacity of a non-catalyzed carbon cathode for Li–O-2 batteries, Electrochem. Solid-State Lett. 15 (4) (2012) A45–A48.
[20] Y.C. Lu, D.G. Kwabi, K.P.C. Yao, J.R. Harding, J. Zhou, L. Zuin, Y. Shao-Horn, The discharge rate capability of rechargeable Li–O_2 batteries, Energy Environ. Sci. 4 (8) (2011) 2999–3007.
[21] W.R. Torres, F. Marchini, A.Y. Tesio, F.J. Williams, E.J., C., EQCM study of the oxygen reduction on Au electrode in DMSO and acetonitrile with LiPF6, J. Electroanal. Chem. (2014) (in preparation).
[22] N. Mozhzhukhina, M.P. Longinotti, H.R. Corti, E.J. Calvo, Lithium preferential solvation in acetonitrile–dimethyl sulfoxide mixtures, J. Phys. Chem. Lett. (2014) (in preparation).
[23] N. Mozhzhukhinaa, R. Semino, G. Zaldivar, D.H. Lariaa, E.J. Calvo, Preferential solvation of lithium ions in acetonitrile-DMSO mixtures, J. Chem. Phys. (2014) (under review at present).
[24] F. Marchini, W. Torres, S. Herrera, A. Tesio, E.J. Calvo, F.J.,W., study of interfacial processes during oxygen electroreduction on Au in DMSO-LiPF6 (2014) (in preparation).